

Influence of Morphological Transition on Crystallization Process in Si

Kazuki WATANABE, Katsuhisa NAGAYAMA and Kazuhiko KURIBAYASHI

Abstract

Using CO₂ laser equipped electro-magnetic levitator, we carried out the crystallization of Si at undercoolings from 0 K to 200 K. From the point of the interface morphologies, the relationship between growth velocities and undercoolings was classified into two regions, I and II, respectively. In region I where the undercooling is approximately less than 100 K, thin plate crystals whose interface consists of faceted plane were observed. In region II, the morphology of growing crystals changed to massive dendrites. Although the interface morphologies look quite different between region I and II, the growth velocities are expressed by two dimensional (2D) nucleation-controlled growth model, and at undercoolings larger than 150 K, the growth velocities asymptotically close to the analysis of the mono-parametric linear kinetics growth model. In this stage, the kinetic coefficient of 0.1 m/sK is equivalent with that derived by the diffusion-controlled growth model. This result means that with increase of undercooling, the rate-determining factor changes from 2D nucleation on the faceted interface to random incorporation of atoms on the rough interface.

1. Introduction

The recent marked increase in the demand for multicrystalline Si solar cells has caused a shortage in Si raw material, since the solar cells had been fabricated using irregular Si for IC/LSI and/or redundant of Si raw material. This unforeseen situation has brought much attention “again” to spherical Si solar cells with diameters of ~1 mm, because the cutting loss required for Si wafer fabrication can be reduced by one fifth.

The first trial of crystal growth of spherical Si was performed by McKee in 1982¹⁾. In his experiment, ingots of Si are melted in a crucible and then ejected into drop-tube to be spherically crystallized during their free fall. Although this process is very simple, the qualities of as-dropped samples were much less than those of single crystals. In order to improve the qualities of as-dropped samples, remelting and regrowing treatment has to be introduced as the post drop-tube process. The cost-up associated with this extra process incurs the disadvantage of spherical Si for use to solar cell.

In recent years, many venture companies in Japan intend to produce the mono-crystalline sphere without any extra processes²⁾⁻⁵⁾. However the control of the falling samples is too difficult for the crystallization condition to be optimized.

In order to simulate the crystallization process in Si during free fall, Aoyama and Kuribayashi⁶⁾ (referred to hereafter as AK) carried out the containerless crystallization of Si using CO₂ laser equipped electro-magnetic levitator. They revealed that at low undercooling less than 100 K plate-like facet crystals grow and

at undercooling larger than 100 K the morphology of solid-liquid interfaces change to dendritic ones^{6),7)}. Nagashio and Kuribayashi⁸⁾ (referred to hereafter as NK) suggested that the plate-like facet crystals are to be grown by the preferential incorporation of atoms into the re-entrant corners formed at the edge of twins (Twin-related Lateral Growth: TrLG), whereas the dendritic crystals are grown by random incorporation of atoms on the non-faceted rough interface (Twin-free Continuous Growth: TfCG).

In rapid solidification of Si into the undercooled melt, AK showed that the relationship between growth velocities and the undercoolings can be analyzed by the dendrite growth model which was proposed by Lipton, Kurz and Trivedi (referred to hereafter as LKT)⁹⁾ (See appendix). However, it is well-known that the interface kinetics (linear kinetics) used in LKT model is strictly based on the assumption that the solid-liquid interface is rough so that atoms can be incorporated at any sites of the interface. In case of Si, the plate-like crystal formed at low undercoolings suggests that the crystal growth is controlled by either the dislocation-assisted spiral growth or the two-dimensional (2D) nucleation models¹⁰⁾. Until now the lack of precise data of growth velocities at low undercoolings has prevented the mechanism of the crystal growth of spherical Si to be clarified. Hence, in the present investigation, precise measurement of growth velocities particularly at relatively low undercooling is aimed to clarify the mechanism of spherical crystallization in Si.

Department of Material Science, School of Engineering, Shibaura Institute of Technology, 3-7-1 Toyosu, Koto-ku, Tokyo 135-8570, Japan
(m210052@sic.shibaura-it.ac.jp)

2. Experimental

Figure 1 shows a schematic illustration of the used electro-magnetic levitator (EML). Undoped 5N Si spheres of 8 mm diameter melted by CO₂ laser were levitated in a 5N Ar gas atmosphere. The sample, after being heated up to approximately 1800 K, was cooled by blowing of 5N He gas to be spontaneously nucleated. **Figure 2** shows the typical profile of temperature vs time measured with a pyrometer (operating wavelength: 900 nm and 1550 nm). After the recalescence, the temperature oscillates in a definite range. In semiconducting Si, since the emissivity (ϵ) of the solid phase is much larger than that of the liquid phase, this temperature oscillation can be attributed the fluctuation of measuring point from liquid phase to solid one and vice versa in levitated sample. Then, in the present experiment, the temperature of the sample, therefore the undercooling, was determined by adjusting ϵ so that the temperature just after the recalescence may be the equilibrium melting temperature of Si.

Growth velocities of samples were measured by means of a

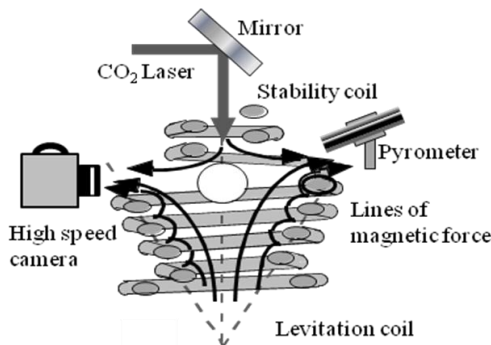


Fig. 1 Schematic illustration of electro-magnetic levitator used in the present investigation.

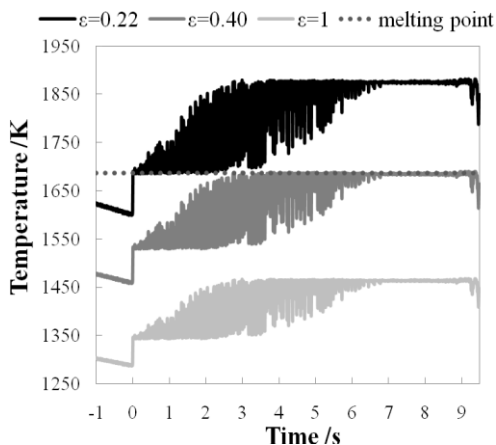


Fig. 2 Typical profile of temperature vs time measured with pyrometer. Temperature of samples was determined by adjusting ϵ so that the temperature just after the recalescence may be the equilibrium melting temperature of Si.

colored high-speed camera (HSC) with a maximum sampling rate of 640,000 frames/s.

3. Results

The HSC images of samples taken during recalescence are shown in **Fig. 3**, where ΔT and V are the undercoolings and the growth velocities, respectively. The dark and bright area respectively shows the undercooled melt and the solidified region. The release of latent heat as well as the difference of emissivities between the solid and the liquid phases enhances the brightness of the solidified region.

In this figure, (a) and (b) are typical images of the interface at low undercoolings, showing anisotropic line-shaped crystal that forms a circumference on the surface of the sample. Note that this circumference is discontinuous, suggesting that the line-shaped crystal is not a “line” crystal located on a surface but a thin-plate crystal that penetrates the sample. On the other hand, at the medium undercooling, it was shown that the solidification front advances massively forming a faceted dendrite (**Fig. 3(c)**). At high undercoolings, as typically shown in **Fig. 3(d)**, dimensions of faceted dendrites were reduced minutely to be a smooth interface.

The growth velocities of samples measured as a function of undercoolings are plotted in **Fig. 4**, where squares and triangles correspond to those of the thin-plate crystal and the faceted dendrite, respectively. Since the growth process of only a pure material is discussed in this article, the constitutional undercooling is ignored. Hence the total undercooling (ΔT) is expressed as the sum of the thermal, curvature and kinetic undercooling. In this figure, the solid and dotted lines correspond to the cases that the kinetic coefficient (μ) is assumed as 0.1 m/sK and 0.02 m/sK, respectively. The physical

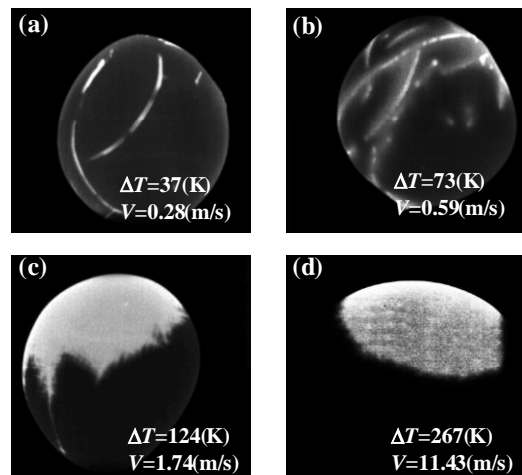


Fig. 3 HSC images of samples taken during recalescence. Dark and bright area respectively shows the undercooled melt and the solidified region.

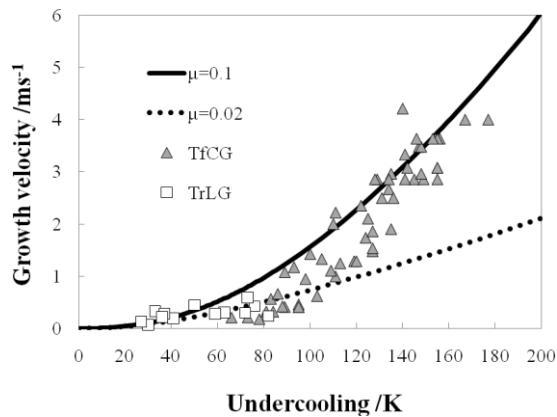


Fig. 4 Growth velocities of samples as a function of undercoolings. Squares and triangles correspond to those of the thin-plate crystal and the faceted dendrite, respectively. Solid and dotted lines correspond to values estimated by the LKT model with the kinetic coefficients, 0.1 m/sK and 0.02 m/sK, respectively.

Table 1 Physical properties used in the calculation

Parameters	Symbol		
Melting temperature	T_m	1687	[K]
Entropy of fusion	ΔS_f	29.99	[J/mol K]
Heat of fusion	ΔH_f	5.06×10^4	[J/mol]
Surface energy	σ	0.438	[J/m ²]
Thermal diffusivity	α	2.35×10^{-5}	[m ² /s]
Specific heat	C_p	25.6	[J/mol K]
Stability constant	σ^*	0.025	
Gibbs Thomson coefficient	Γ	1.46×10^{-2}	[mol K/m ²]

parameters used in the calculation are listed in **Table 1**.

It looks that V vs ΔT for thin-plate crystals can be fitted by μ of 0.02 m/sK. For faceted dendrites, however, it is unable to express V vs ΔT with a mono-parametric μ , suggesting a change of the mechanism of the interface kinetics.

4. Discussion

AK shows that the relationship between growth velocities and undercoolings in Si can be well expressed by LKT model with the mono-parametric interface kinetics, although the morphologies of crystal-melt interface drastically changes from thin-plate crystal to faceted dendrite at the transient stage from region I to II. NK suggested that the thin-plate crystals are TrLG, which grow at the re-entrant corner formed at the edge of the twin boundaries, and TfCG is by random incorporation of atoms on the non-faceted rough interface. If their suggestion is true, the kinetics of the crystal growth is different from the linear interface kinetics shown in the LKT model.

It is well known that in faceted material the crystal growth is controlled by either the dislocation-assisted spiral growth or the two-dimensional (2D) nucleation models. These mechanisms have to be the case in the crystal growth into undercooled melts. On the basis of this idea, we incorporated other types of interfacial kinetics into LKT model so as to fit with the experimental data. One is the quadratic kinetics equation:

$$V = \alpha(\Delta T_k)^2$$

and the other the exponential kinetics equation:

$$V = \beta \exp\left(-\frac{E}{k_B \Delta T_k}\right)$$

Figure 5 shows the results for these two cases, where α , β and E/k_B are optimized to 3.0×10^{-3} m/s·K², 7.0×10^5 and 3.5×10^2 K, respectively.

As clearly shown in this figure, the exponential kinetics well fitted to the experimental data. At relatively high undercoolings typically $\Delta T > 150$ K, it looks that the experimental data asymptotically close to the analysis with the linear interface kinetics, the coefficient of which is that of Wilson-Frenkel model (see Appendix). These results suggest that the crystal growth at relatively low and medium undercoolings is controlled by the 2D nucleation not only in TrLG but also in TfCG, and at relatively high undercooling by diffusion-controlled linear kinetics.

5. Conclusion

In containerless crystallization of Si, depending on the undercooling level, various morphologies of crystal-melt interface appeared: At relative low undercooling, the morphology of growing crystal was like a thin-plate (Twin-related Lateral Growth: TrLG), whereas at medium undercooling, a massive dendrite (Twin-free Continuous Growth: TfCG). The experimental data of growth velocities in

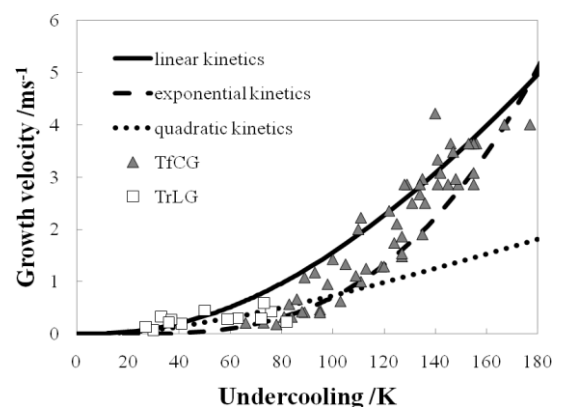


Fig. 5 Growth velocities of samples as a function of undercoolings. Solid, broken and dotted lines correspond to values estimated by the modified LKT model, each of which is linear, exponential and quadratic kinetics, respectively.

the region from relatively low undercooling to medium undercooling well fitted to the dendrite growth model incorporating the exponential kinetics. LKT model which incorporate the mono-parametric linear kinetics fitted to the data at relative high undercooling, where the kinetic coefficient μ is nearly equal to that derived with Wilson-Frenkel model. This result suggests that not only TrLG but also TfCG is controlled by the 2D nucleation rate.

References

- 1) W. R. McKee, IEEE Trans. Components, Hybrids, and Manufacturing Tech. **5**(1982) 336-341.
- 2) T. Minemoto, C. Okamoto, S. Omae, M. Murozono, H. Takakura, and Y. Hamakawa: Jpn. J. Appl. Phys., **44**(2005) 4820-4824.
- 3) K. Taira, N. Kogo, H. Kikuchi, N. Kumagai, N. Kuratani, I. Inagawa, S. Imoto, J. Nakata and M. Biancardo: Tech. Dig., PVSEC-15, (2005) 202-203.
- 4) S. Masuda, K. Takagi, Y.-S. Kang and A. Kawasaki: J. Jpn. Soc. Powder Metallurgy, **51** (2004) 646-654.
- 5) W. Dong, K. Takagi, S. Masuda, and A. Kawasaki: J. Jpn. Soc. Powder Metallurgy, **53** (2006) 346-351.
- 6) T. Aoyama and K. Kuribayashi: Acta mater., **48**(2000) 3739-3744.
- 7) T. Aoyama, Y. Takamura and K. Kuribayashi: Metall. Mater. Trans. A, **30A** (1999) 1333-1339.
- 8) K. Nagashio and K. Kuribayashi: Acta mater., **53**(2005) 3021-3029.
- 9) J. Lipton, W. Kurz and R. Trivedi: Acta metall., **35**(1987) 957-964.
- 10) K. F. Kelton, Solid State Physics, **45**(1991) 75-177.

Appendix

LKT model

The bulk undercooling ΔT for pure material is given by

$$\Delta T = \Delta T_i + \Delta T_r + \Delta T_k \quad (\text{A1})$$

where ΔT_i is the thermal undercooling given by

$$\Delta T_i = \frac{\Delta H_f}{C_p} \text{Iv}(P_i) \quad (\text{A2})$$

for the case in which the shape of the growth front can be approximated as an elliptical paraboloid. In this equation, ΔH_f is the enthalpy of fusion, C_p is the specific heat of the melt at constant pressure, and $\text{Iv}(P_i)$ is the Ivantsov function given by

$$\text{Iv}(P_i) = P_i \exp(P_i) \int_{P_i}^{\infty} \frac{\exp(-P_i)}{P_i} dP_i \quad (\text{A3})$$

where $P_i = VR/2a_i$ denotes the thermal Peclet number, R the radius of the growth front, and a_i the thermal diffusivity.

In Eq. (A1), ΔT_r , the curvature undercooling due to the Gibbs-Thomson effect, is expressed by

$$\Delta T_r = \frac{2\Gamma}{R} \quad (\text{A4})$$

where $\Gamma = \sigma/\Delta S_f$ is the Gibbs-Thomson coefficient.

The kinetic undercooling ΔT_k is given by

$$\Delta T_k = V/\mu \quad (\text{A5})$$

where μ is the kinetic coefficient. According to the marginal stability analysis, the radius of the growth front that is assumed to be equal to the wavelength of a critical perturbation of a planar interface λ_l is derived as

$$R = \frac{\Gamma/\sigma^*}{P_i \frac{\Delta H_f}{C_p} \left(1 - \frac{1}{\sqrt{\sigma^* P_i^2}} \right)} \quad (\text{A6})$$

where σ^* , a stability constant, was approximately derived to be 0.025 using the marginal stability criterion.

Wilson-Frenkel Model

Under the assumption of diffusion-limited crystal growth, the growth velocity V is given by the difference between the rates of attachment and detachment of growth units at a growth front

$$V = a \nu \exp\left(-\frac{\Delta S_f}{k_B}\right) \exp\left(-\frac{E_D}{k_B T}\right) \left[1 - \exp\left(-\frac{\Delta G}{k_B T}\right) \right] \quad (\text{A7})$$

where a , ν and E_D are the interatomic distance, the atomic vibration frequency and the activation energy for atomic diffusion in the liquid phase. The first exponential function is due to the difference in the numbers of states between the solid and liquid phases, that is, $\exp(-\Delta S_f/k_B) = W_s/W_l$, where W_s and W_l are the numbers of states in the solid and the liquid phases, respectively.

If ΔG can be assumed to be sufficiently small for the higher-order term in the series expansion of the exponential function in the bracket to be ignored, a kinetic coefficient $\mu = V/\Delta T_k$ is given by

$$\mu = \frac{D}{aT} \frac{\Delta S_f}{k_B} \exp\left(-\frac{\Delta S_f}{k_B}\right) \quad (\text{A8})$$

where ΔT_k denotes kinetic undercooling at an interface and D is the diffusion coefficient in the liquid phase. The kinetic coefficient passes through a maximum at $\Delta S_f/k_B = 1$. In Si, $\Delta S_f/k_B$ is approximately 3.6. Therefore, if D and a are respectively assumed as $1.0 \times 10^{-9} \text{ m}^2/\text{s}$ and $2.5 \times 10^{-10} \text{ m}$, μ can be derived as approximately 0.1 m/sK.

(Received 7 Oct. 2010; Accepted 14 Jun. 2011)